

## Article

# Performance of a Thermodynamic Model for Predicting Inorganic Aerosols in the Southeastern U.S.

Bin Cheng <sup>1</sup>, Lingjuan Wang-Li <sup>1,\*</sup> , John Classen <sup>1</sup>  and Peter Bloomfield <sup>2</sup>

<sup>1</sup> Department of Biological and Agricultural Engineering, North Carolina State University, Raleigh, NC 27695, USA

<sup>2</sup> Department of Statistics, North Carolina State University, Raleigh, NC 27695, USA

\* Correspondence: lwang5@ncsu.edu; Tel.: +1-919-515-6762; Fax: +1-919-515-7760

**Abstract:** Fine particulate matter (i.e., PM<sub>2.5</sub>) has gained intensive attention due to its adverse health and visibility degradation effects. As a significant fraction of atmospheric PM<sub>2.5</sub>, secondary inorganic PM<sub>2.5</sub> may be formed through the gas-phase ammonia (NH<sub>3</sub>) and particle-phase ammonium (NH<sub>4</sub><sup>+</sup>) partitioning. While partitioning of NH<sub>3</sub>-NH<sub>4</sub><sup>+</sup> may be simulated using a thermodynamic equilibrium model, disagreement between model predictions and measurements have been realized. In addition, the applicability of the model under different conditions has not been well studied. This research aims to investigate the applicability of a thermodynamic equilibrium model, ISORROPIA II, under different atmospheric conditions and geographic locations. Based upon the field measurements at the Southeastern Aerosol Research and Characterization (SEARCH) network, the performance of ISORROPIA II was assessed under different temperature (T), relative humidity (RH), and model setups in urban and rural locations. The impact of organic aerosol (OA) on the partitioning of NH<sub>3</sub>-NH<sub>4</sub><sup>+</sup> was also evaluated. Results of this research indicate that the inclusion of non-volatile cations (NVCs) in the model input is necessary to improve the model performance. Under high T (>10 °C) and low RH (<60%) conditions, ISORROPIA II tends to overpredict nitric acid (HNO<sub>3</sub>) concentration and underpredict nitrate (NO<sub>3</sub><sup>-</sup>) concentration. The predominance of one phase of semi-volatile compound leads to low accuracy in the model prediction of the other phase. The model with stable and metastable setups may also perform differently under different T-RH conditions. Metastable model setup might perform better under high T (>10 °C) and low RH (<60%) conditions, while stable model setup might perform better under low T (<5 °C) conditions. Both model setups have consistent performance when RH is greater than 83%. Future studies using ISORROPIA II for the prediction of NH<sub>3</sub>-NH<sub>4</sub><sup>+</sup> partitioning should consider the inclusion of NVCs, the under/over prediction of NO<sub>3</sub><sup>-</sup>/HNO<sub>3</sub>, the selection of stable/metastable model setups under different T-RH conditions, and spatiotemporal variations of inorganic PM<sub>2.5</sub> chemical compositions.

**Keywords:** gas-particle partitioning; inorganic PM<sub>2.5</sub>; thermodynamic equilibrium



**Citation:** Cheng, B.; Wang-Li, L.; Classen, J.; Bloomfield, P. Performance of a Thermodynamic Model for Predicting Inorganic Aerosols in the Southeastern U.S. *Atmosphere* **2022**, *13*, 1977. <https://doi.org/10.3390/atmos13121977>

Academic Editor: László Bencs

Received: 1 November 2022

Accepted: 24 November 2022

Published: 26 November 2022

**Publisher's Note:** MDPI stays neutral with regard to jurisdictional claims in published maps and institutional affiliations.



**Copyright:** © 2022 by the authors. Licensee MDPI, Basel, Switzerland. This article is an open access article distributed under the terms and conditions of the Creative Commons Attribution (CC BY) license (<https://creativecommons.org/licenses/by/4.0/>).

## 1. Introduction

Fine particulate matter with aerodynamic diameter less than 2.5 μm (i.e., PM<sub>2.5</sub>) has gained attention due to its adverse health effects, visibility degradation, and the impacts on the Earth's ecosystems and radiative balance [1–3]. Secondary inorganic PM<sub>2.5</sub> (iPM<sub>2.5</sub>) constitutes a significant fraction of atmospheric PM<sub>2.5</sub> mass concentration and the chemistry of secondary iPM<sub>2.5</sub> formation has been investigated for decades [4–7]. The formation of the secondary iPM<sub>2.5</sub> may be characterized by thermodynamic equilibrium of gas-phase ammonia (NH<sub>3</sub>) and particle-phase ammonium (NH<sub>4</sub><sup>+</sup>) partitioning [8,9]. It is important to establish a holistic understanding of the formation of secondary iPM<sub>2.5</sub> such that the regional impact of iPM<sub>2.5</sub> may be fully understood. Secondary iPM<sub>2.5</sub> is usually formed through chemical reactions between different basic and acidic gases such as NH<sub>3</sub>, nitric acid (HNO<sub>3</sub>), and sulfuric acid (H<sub>2</sub>SO<sub>4</sub>). In general, NH<sub>3</sub> gas is directly emitted, while HNO<sub>3</sub>

and  $\text{H}_2\text{SO}_4$  mainly form through (photo)chemical reactions during atmospheric transformation of sulfur dioxide ( $\text{SO}_2$ ) and nitrogen oxides ( $\text{NO}_x$ ) ( $\text{NO}_x = \text{NO} + \text{NO}_2$ ). It was reported that  $\text{iPM}_{2.5}$  mainly consists of ammonium nitrate ( $\text{NH}_4\text{NO}_3$ ), ammonium sulfate ( $(\text{NH}_4)_2\text{SO}_4$ ), ammonium bisulfate ( $\text{NH}_4\text{HSO}_4$ ), and ammonium chloride ( $\text{NH}_4\text{Cl}$ ) [10–16]; the latest research found that  $\text{NH}_4\text{HSO}_4$  is the dominant component for  $\text{SO}_4^{2-}$  aerosols due to acidic properties of the particles [17]. The partitioning of total ammonia ( $\text{NH}_3 + \text{NH}_4^+$ ) into gas and particle phase is usually assumed to be in the thermodynamic equilibrium state such that thermodynamic models can be used to estimate the physical phases (gas, liquid, solid) and interactions of different precursor gases of  $\text{iPM}_{2.5}$  [18–20]. However, the non-equilibrium state may exist in ambient air due to surface heterogeneity [21], the mass transport limitation between different sizes of particles [22], and the long timescale to reach equilibrium state for super-micron particles [23]. Consequently, the applicability of thermodynamic equilibrium theory for modelling the  $\text{NH}_3\text{-NH}_4^+$  partitioning may lead to erroneous results under certain atmospheric conditions. As a widely used thermodynamic equilibrium model, ISORROPIA II has been coupled to large-scale chemical transport model (CTM) to predict the concentrations of secondary  $\text{iPM}_{2.5}$  at equilibrium state. In this study, we carry out comprehensive evaluation of the applicability of the ISORROPIA II model for predicting inorganic aerosols.

The default assumption made in the thermodynamic equilibrium model is that the gas and particle system is in a chemical equilibrium state, i.e., the total free energy of the system is minimized [8]. The ISORROPIA II [24] is one of the commonly used thermodynamic models, in which gas-particle partitioning phenomenon and the impacts of temperature (T) and relative humidity (RH) are incorporated. The mutual deliquescence region and hysteresis phenomenon are both resolved in the model. In addition, compared with other thermodynamic models, ISORROPIA II is more computationally efficient with stable performance [24–27]. Input data required by the ISORROPIA II include the concentrations of  $\text{NH}_3$ ,  $\text{HNO}_3$ ,  $\text{H}_2\text{SO}_4$ , hydrochloric acid (HCl) in both gas and particle phases, T and RH. Two types of problem (forward and backward) can be solved by ISORROPIA II [28]. The input data for forward problem include total concentrations of precursor gases existing both in gas and particle phases. The input data for backward problem include the concentrations of precursor gases exclusively in particle phase. In addition, thermodynamically stable and metastable states can be set by the user to adapt to different application scenarios. The difference between these two states reflects if the salts in the solution will precipitate when super saturation state is achieved. For thermodynamically stable states, the salts will precipitate when super saturation is achieved, while for metastable states, the salts remain in the aqueous phase. The outputs of the model include the concentrations of gases,  $\text{iPM}_{2.5}$  chemical compositions, hydrogen ion, and water content at chemical equilibrium state for both forward and backward problems.

The ISORROPIA II model assumes that the thermodynamic equilibrium is established instantaneously, and the equilibrium state could also be kinetically approached, which was done in some Chemical Transport Model (CTM) applications [29,30]. To prove the validity of this assumption, the timescales to reach thermodynamic equilibrium state were assessed by different researchers [31,32]. The theoretical calculations revealed that it takes around 5–30 min for submicron ( $\text{PM}_1$ ) and more than 1 h for super-micron ( $\text{PM}_{1-2.5}$ ) aerosols to reach equilibrium state. Therefore, the application of equilibrium models (e.g., ISORROPIA II) to timescales shorter than the equilibrium time would be problematic. In addition, the field sampling with long integration time may not be able to detect the variation of gas- and particle-phase pollutants caused by dramatic changes of ambient conditions. If ambient conditions and inorganic aerosol compositions are variable on timescales shorter than the sampling timescale, then that could be problematic for an equilibrium model application, which should be calculating all the individual equilibrium states rather than an average over all states.

Time resolution of the concentrations of  $\text{iPM}_{2.5}$  and its precursor gases varied in different field studies from several minutes to 24 h due to the differences in the measurement

instruments and techniques. Zhang et al., (2002), Yu et al., (2005), and Fountoukis et al., (2009) used 5–6 min measurements to assess the performance of ISORROPIA II [32–34]; Yu et al., (2005) and Takahama et al., (2004) used 1–3 h measurements to check the prediction skill of ISORROPIA II [34,35]; Moya et al., (2001), Yu et al., (2005), and Goetz et al., (2008) used 6–24 h measurements to investigate the performance of ISORROPIA II [34,36,37]. The measurements with 6 to 24 h time resolution may not be suitable to assess the model prediction skill because the greater time scale loses the resolution to detect the impact of ambient condition changes on the  $\text{NH}_3$ - $\text{NH}_4^+$  partitioning process.

Factors influencing the gas-particle system equilibrium state include ambient meteorological condition [38], surface heterogeneity and multiphase chemistry [21], and organic aerosols coating inorganic aerosols [39,40]. Thus, the application of thermodynamic models such as ISORROPIA II may also be affected by those factors [22]. Thermodynamic equilibrium models predict the molar ratio  $R$  ( $R = ([\text{NH}_4^+] - [\text{NO}_3^-] - [\text{Cl}^-]) / [\text{SO}_4^{2-}]$ ) to be 2 when  $\text{NH}_3$  is abundant compared to acidic gases, corresponding to the stoichiometry of  $(\text{NH}_4)_2\text{SO}_4$ . Research conducted by Li et al., (2014a, b) detected the high concentration of  $\text{NH}_3$  gas near the source region [41,42]. It was observed that the mean  $R$  was 1.75, which is less than 2, although this ratio should be close to 2 under high  $\text{NH}_3$  concentration environments. Further investigation suggested that wind speed may affect the local thermodynamic equilibrium status as the time for establishing such equilibrium may exceed the time needed for transporting  $\text{NH}_3$ -laden air parcels from emission sources under high wind speed. The concentrations of  $\text{iPM}_{2.5}$  chemical compositions and precursor gases were measured at an agricultural site located in an area impacted by the  $\text{NH}_3$  emissions from intensive animal production activities and fertilizer application [38]. It was also discovered that the mean  $R$  was approximately 1.43. The high  $\text{NH}_3$  concentrations at the site present a potential to react with acidic gases, and the abundant  $\text{NH}_3$  should render molar ratio  $R$  close to 2. Walker et al., (2006) noted that the possible reason for the low molar ratio  $R$  may be due to the non-equilibrium state of the  $\text{NH}_4^+$ - $\text{NO}_3^-$ - $\text{SO}_4^{2-}$  system; the mass transport between gaseous  $\text{NH}_3$  and particles may limit the protonation of  $\text{NH}_3$  by  $\text{H}_2\text{SO}_4$  [38]. Although the applicability of ISORROPIA II in rural area with high  $\text{NH}_3$  concentrations was not fully assessed in the research, the ISORROPIA II model was utilized to investigate the responses of secondary  $\text{iPM}_{2.5}$  to the changes of precursor gases. Further investigation should be conducted to advance our understanding on the thermodynamic equilibrium assumption.

The impact of organic matter on the chemistry of  $\text{NH}_3$  and acidic gas  $\text{H}_2\text{SO}_4$  involves complex processes, and, in the literature, there are two contradictory explanations. Liggio et al., (2011) investigated the time to achieve equilibrium state in the system of  $\text{NH}_3$ - $\text{H}_2\text{SO}_4$ -organics [43]. In a closed chamber, particle-free ambient air was exposed to  $\text{H}_2\text{SO}_4$  aerosols. The initial molar ratio of total  $\text{NH}_3$ /total  $\text{H}_2\text{SO}_4$  was set at various values and the steady  $\text{NH}_4^+/\text{SO}_4^{2-}$  molar ratio was treated as the equilibrium indicator. The comparison of equilibrium time between the organic-free system and the organic-rich system indicated the delay effect of organics on the  $\text{NH}_3$  uptake to  $\text{H}_2\text{SO}_4$  particles. The inorganic particles may be coated by organic materials, which leads to a long equilibrium time, i.e., hours instead of minutes. Silvern et al., (2017) compared the  $[\text{NH}_4^+]/[\text{SO}_4^{2-}]$  in the air with the values in rainwater in the eastern U.S. The results indicated that not all the  $\text{SO}_4^{2-}$  was in the form of  $(\text{NH}_4)_2\text{SO}_4$ , even with abundant  $\text{NH}_3$  in ambient air [39]. The possible reason is that the organic aerosol (OA) coating on the inorganic particles may hinder the reaction of  $\text{NH}_3$  and acidic gases. On the other hand, Pye et al., (2018) noted that the organic coatings may not be needed to explain the  $[\text{NH}_4^+]/[\text{SO}_4^{2-}]$  because the Chemical Speciation Network (CSN) contains measurement artifacts leading to ammonium volatilization, and aerosol mass spectrometer (AMS) measurements also include organosulfates in total sulfate [44]. Furthermore, Guo et al., (2018) challenged the ability of organic film to retard  $\text{NH}_3$  uptake [45]. In this newer research, the OA/ $\text{PM}_{2.5}$  mass fraction was utilized to represent the thickness of organic film. No significant relationship between the measured molar ratio of

$[\text{NH}_4^+]/[\text{SO}_4^{2-}]$  and  $\text{OA}/\text{PM}_{2.5}$  mass fraction was observed. This finding may challenge the ability of organic film to retard  $\text{NH}_3$  uptake.

The ISORROPIA II model simulates the  $\text{K}^+ - \text{Ca}^{2+} - \text{Mg}^{2+} - \text{NH}_4^+ - \text{Na}^+ - \text{SO}_4^{2-} - \text{NO}_3^- - \text{Cl}^- - \text{H}_2\text{O}$  system; thus, the ISORROPIA model has been used to estimate particle pH due to the lack of operational techniques for direct particle pH measurements [17,46]. In addition, oftentimes, the nonvolatile cations (NVCs) such as potassium ( $\text{K}^+$ ), calcium ( $\text{Ca}^{2+}$ ), magnesium ( $\text{Mg}^{2+}$ ), and sodium ( $\text{Na}^+$ ) may not be monitored due to the limitation of measurement instruments and techniques. Fountoukis et al., (2009) and Guo et al., (2018) observed that the inclusion of measured  $\text{Na}^+$  to the model input significantly improved the performance of ISORROPIA II in reproducing the gas-phase and particle-phase pollutants [32,45].

In this study, we explore impacts of the factors, e.g., organic materials, and ambient T and RH, on the performance of the ISORROPIA II model with an aim to identify the possible reasons to the underestimations or overestimations in the concentrations of gas-phase and particle-phase species.

## 2. Materials and Methods

### 2.1. Monitoring Network Description

The Southeastern Aerosol Research and Characterization (SEARCH) Network is a long-term air quality monitoring network established in the southeastern U.S. (AL, FL, GA, and MS) [47]. The network provides high-quality field measurements of  $\text{PM}_{2.5}$  mass and chemical compositions. More specifically, the continuous measurements of  $\text{iPM}_{2.5}$  chemical compositions and its precursor gases provides information with high time resolution to investigate the partitioning of gas- and particle-phase pollutants at eight sites covering agricultural rural areas and urban regions.

Under the SEARCH, the concentrations of  $\text{iPM}_{2.5}$  chemical compositions and its precursor gases were measured at four paired urban/nonurban sites, named as JST/YRK, BHM/CTR, GFP/OAK, and PNS/OLF. The measurements started from 1998/1999 and ended in 2016. These eight monitoring sites are shown in Figure 1.

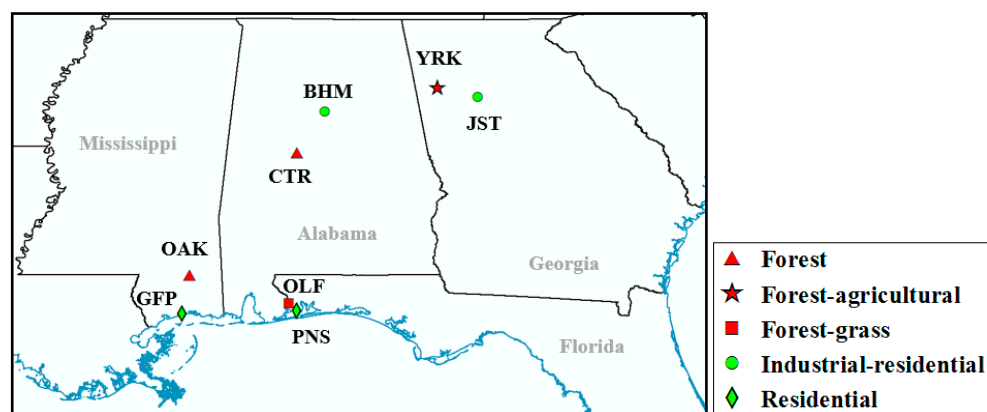


**Figure 1.** The geographical locations of the eight monitoring sites under the SEARCH (Green label indicates urban sites; red label indicates rural or suburban sites).

The onsite measurements provided processed 1 h average concentrations of precursor gases,  $\text{iPM}_{2.5}$  chemical compositions, and meteorological conditions. In addition, the 24 h average measurements of  $\text{iPM}_{2.5}$  chemical compositions were also performed. The details of the measurements made at the eight sites are reported in [48,49] and summarized in Table 1.

**Table 1.** Continuous and discrete field measurements at the eight sites.

Observable	Technique	Max Resolution	Detection Limit (ppb or $\mu\text{g m}^{-3}$ )
Gases			
NO	CL <sup>a</sup>	1 min	0.05
NO <sub>2</sub>	Photolysis/CL	1 min	0.1
HNO <sub>3</sub>	Denuder/Mo reduction/CL	1 min	0.1
NO <sub>y</sub>	Mo reduction/CL	1 min	0.1
SO <sub>2</sub>	UV-fluorescence	1 min	0.2
NH <sub>3</sub>	Denuder/Pt oxidation/CL	5 min	0.2
iPM <sub>2.5</sub> chemical compositions			
SO <sub>4</sub> <sup>2-</sup>	Fe reduction/UV-fluorescence	5 min	0.4
NO <sub>3</sub> <sup>-</sup>	Filter/Mo reduction/CL	5 min	0.2
NH <sub>4</sub> <sup>+</sup>	Filter/Pt oxidation/CL	5 min	0.1
Meteorological conditions			
T/RH/SR <sup>b</sup> /BP <sup>c</sup>	Various	1 min	NA
WS <sup>d</sup> /WD <sup>e</sup> /Precipitation	Various	1 min	NA
Discrete iPM <sub>2.5</sub> chemical compositions			
NO <sub>3</sub> <sup>-</sup>	Teflon filter + IC <sup>f</sup>	24 h	0.01
Volatile NO <sub>3</sub> <sup>-</sup>	Nylon filter + IC	24 h	0.02
NH <sub>4</sub> <sup>+</sup>	Teflon filter + AC <sup>g</sup>	24 h	0.03
Volatile NH <sub>4</sub> <sup>+</sup>	Citric acid annular denuder + AC	24 h	0.04
SO <sub>4</sub> <sup>2-</sup>	Teflon filter + IC	24 h	0.05
K <sup>+</sup> -Ca <sup>2+</sup> -Mg <sup>2+</sup> -Na <sup>+</sup>	Teflon filter + ICP-MS <sup>h</sup>	24 h	NA <sup>i</sup>

<sup>a</sup> CL: chemiluminescence; <sup>b</sup> SR: solar radiation; <sup>c</sup> BP: barometric pressure; <sup>d</sup> WS: wind speed; <sup>e</sup> WD: wind direction; <sup>f</sup> IC: ion chromatography; <sup>g</sup> AC: automated colorimetry; <sup>h</sup> ICP-MS: inductively coupled plasma mass spectrometry; <sup>i</sup> NA: not applicable.

## 2.2. Data Reduction and Processing

Some of the reported gas- and particle-phase measurements were found to be negative or below the instrument's detection limit. All the negative values were excluded from the analysis, while those values below the detection limits were included in the data analysis [50,51].

During the SEARCH data collection period, rain events happened that led to pollutant wet depositions. The precipitation led to a rapid decrease in the concentrations of gas- and particle-phase pollutants. Thus, the hourly and daily measurements in rain events are not suitable to assess the performance of the thermodynamic model. In data reduction process, the hours and days with precipitation were flagged and excluded from the analysis.

## 2.3. Thermodynamic Model Assessment

We explore the impact of factors including ambient T and RH, stable/metastable model setups, and NVCs on the performance of ISORROPIA II. Comparisons of model predicted concentrations and measurements were performed to check the over or underestimations of ISORROPIA II under various conditions and to identify the possible reasons. In addition, the impact of OA on the thermodynamic equilibrium partitioning of NH<sub>3</sub>-NH<sub>4</sub><sup>+</sup> was evaluated as well.

The impacts of T and RH on the model performance are assessed using the following experimental design. The T and RH scenarios are broken down into various 5 °C T × 10% RH conditions; under each condition, the model-predicted concentrations of NH<sub>3</sub>, NH<sub>4</sub><sup>+</sup>, HNO<sub>3</sub>, NO<sub>3</sub><sup>-</sup>, and iPM<sub>2.5</sub> (SO<sub>4</sub><sup>2-</sup> + NH<sub>4</sub><sup>+</sup> + NO<sub>3</sub><sup>-</sup>) were assessed against hourly measurements of gas-phase and particle-phase pollutants.

The gas-phase NH<sub>3</sub> and HNO<sub>3</sub> molar fractions under different T-RH conditions were also analyzed. The gas-phase NH<sub>3</sub> molar fraction ( $[\text{NH}_3]/[\text{NH}_x]$ ) and gas-phase HNO<sub>3</sub> molar fraction ( $[\text{HNO}_3]/[\text{TN}]$ ) are defined in Equations (1) and (2):

$$[\text{NH}_3]/[\text{NH}_x] = \frac{[\text{NH}_3]}{[\text{NH}_3] + [\text{NH}_4^+]} \quad (1)$$

$$[\text{HNO}_3]/[\text{TN}] = \frac{[\text{HNO}_3]}{[\text{HNO}_3] + [\text{NO}_3^-]} \quad (2)$$

where  $[\text{NH}_x]$  is the sum of molar concentrations ( $\mu\text{mol m}^{-3}$ ) of gas-phase  $\text{NH}_3$  and particle-phase  $\text{NH}_4^+$ , and  $[\text{TN}]$  is the sum of molar concentrations ( $\mu\text{mol m}^{-3}$ ) of gas-phase  $\text{HNO}_3$  and particle-phase  $\text{NO}_3^-$ .

The ISORROPIA II is usually utilized to predict the gas-particle partitioning given the concentrations of precursor gases, thus forward mode is used as default in this study. The performance of ISORROPIA II with thermodynamically stable and metastable setups under different T and RH conditions was assessed by comparing forward model predictions with field measurements to check the applicability of the model for predicting inorganic aerosols under different conditions.

The hourly measurements only included the concentrations of  $\text{NH}_3$ ,  $\text{NH}_4^+$ ,  $\text{HNO}_3$ ,  $\text{NO}_3^-$ , and  $\text{SO}_4^{2-}$ . The discrepancies in the predictions of gas- and particle-phase pollutants may be due to the lack of other cations/anions measurements. Thus, the model performances of ISORROPIA II in simulating  $\text{NH}_3$ ,  $\text{HNO}_3$ ,  $\text{NH}_4^+$ , and  $\text{NO}_3^-$  under different gas ratios (GR) and measured charge balances were analysed. The GR characterizes the potential reaction of  $\text{NH}_3$  and acidic gases, and measured charge balance is the molar difference of cation ( $\text{NH}_4^+$ ) and anions ( $\text{SO}_4^{2-}$  and  $\text{NO}_3^-$ ). More specifically, GR and charge balance can be defined as Equations (3) and (4):

$$\text{GR} = \frac{[\text{TA}] - 2[\text{TS}]}{[\text{TN}]} \quad (3)$$

$$\text{Measured charge balance} = [\text{NH}_4^+] - 2 \times [\text{SO}_4^{2-}] - [\text{NO}_3^-] \quad (4)$$

where TA is total available ammonia ( $\text{NH}_3 + \text{NH}_4^+$ ), TS is total sulfate ( $\text{H}_2\text{SO}_4 + \text{HSO}_4^- + \text{SO}_4^{2-}$ ), and TN is total nitrate ( $\text{HNO}_3 + \text{NO}_3^-$ ).

In terms of the impact of NVCs on the model performance, only 24 h average data of  $\text{K}^+$ ,  $\text{Ca}^{2+}$ ,  $\text{Mg}^{2+}$ , and  $\text{Na}^+$  were available under the SEARCH Network. Thus, 24 h average data of  $\text{iPM}_{2.5}$  chemical composition and its precursor gases were used to assess the impact of NVCs inclusion/exclusion on the model performance. For each site, two datasets were used to run ISORROPIA II: one was  $\text{NH}_3\text{-NH}_4^+\text{-HNO}_3\text{-NO}_3^-\text{-SO}_4^{2-}$  system, the other one was  $\text{Ca}^{2+}\text{-Mg}^{2+}\text{-K}^+\text{-Na}^+\text{-HCl-Cl}^-\text{-NH}_3\text{-NH}_4^+\text{-HNO}_3\text{-NO}_3^-\text{-SO}_4^{2-}$  system.

If  $\text{iPM}_{2.5}$  may be coated with organic film, retarding the uptake of  $\text{NH}_3$  to react with  $\text{H}_2\text{SO}_4$ , then the higher OA/ $\text{SO}_4^{2-}$  mass ratio may lead to lower probability of the reaction between  $\text{NH}_3$  and  $\text{H}_2\text{SO}_4$  [43]. The reaction of  $\text{H}_2\text{SO}_4$  and  $\text{NH}_3$  was characterized by molar ratio R, Equation (5):

$$R = \frac{[\text{NH}_4^+] - [\text{NO}_3^-] - [\text{Cl}^-]}{[\text{SO}_4^{2-}]} \quad (5)$$

The postulated organic film hypothesis was examined by testing if there was a significant correlation between molar ratio R and OA/ $\text{SO}_4^{2-}$  mass ratio. The negative correlation may indicate the organic film hypothesis, while no correlation may challenge the organic film hypothesis.

The pH was calculated to study the acidity of the inorganic aerosol:

$$\text{pH} = -\log_{10} \frac{1000\gamma_{\text{H}^+} + H_{\text{air}}^+}{W} \quad (6)$$

where  $\gamma_{\text{H}^+}$  is the hydronium ion activity coefficient, which is set as unity,  $H_{\text{air}}^+$  ( $\mu\text{g m}^{-3}$ ) is the hydronium ion concentration in volume of air, and W ( $\mu\text{g m}^{-3}$ ) is particle water concentration associated with inorganic aerosol. Both  $H_{\text{air}}^+$  and W are from the ISORROPIA II model output.

#### 2.4. Statistical Tests of the Model Performance Assessment

Following the approaches by [32,52,53], four parameters were used to evaluate the performance of the ISORROPIA II model. The four parameters' criteria values for acceptable model performance and associated meanings are as follows (the bracket means averaging;  $C_o$  and  $C_p$  denote measured and predicted concentration):

1. Fraction of predictions falls in a factor of two of observations ( $Fa_2$ ): the fraction of data with  $0.5 \leq \frac{C_p}{C_o} \leq 2.0$  ( $Fa_2 \geq 0.8$ ).

The perfect model should have  $Fa_2 = 1$  acceptable model performance should have  $Fa_2$  greater than 0.8.

2. Normalized mean square error (NMSE):  $NMSE = \frac{[(C_o - C_p)^2]}{[C_o] \times [C_p]}$  ( $NMSE \leq 0.5$ ).

The NMSE measures the scatter of the data and indicates both systematic and random errors. The perfect model should have  $NMSE = 0$  and the acceptable model performance should have  $NMSE$  less than 0.5.

3. Fractional bias (FB):  $FB = \frac{2 \times ([C_p] - [C_o])}{[C_o] + [C_p]}$  ( $-0.5 \leq FB \leq 0.5$ ).

FB is symmetrical and bounded between  $-2$  and  $2$ ;  $FB = -2$  indicates extremely underprediction and  $FB = 2$  indicates extremely overprediction. The perfect model should have  $FB = 0$ . The acceptable model performance should have  $FB$  in the range between  $-0.5$  and  $0.5$ .

4. Geometric mean bias (MG):  $MG = \exp([\ln C_p] - [\ln C_o])$  ( $0.75 \leq MG \leq 1.25$ ).

The MG is suitable to assess datasets with a large range of concentrations, and the perfect model should have  $MG = 1$ . The acceptable model performance should have  $MG$  in the range between  $0.75$  and  $1.25$ . Both  $FB$  and  $MG$  measure the mean bias of the prediction and indicate systematic errors. The  $FB$  and  $MG$  can also be used to check the over or underprediction of the ISORROPIA II model;  $FB > 0$  and  $MG > 1$  indicate overprediction and  $FB < 0$  and  $MG < 1$  indicate underprediction. In addition,  $NMSE$  and  $MG$  are not defined for zero values. In this research,  $FB$  was used as a proxy for the model performance assessment parameter.

### 3. Results and Discussion

#### 3.1. Applicability of ISORROPIA II in the Predictions of Gas- and Particle-Phase Pollutants

The ISORROPIA II model performance evaluation at the YRK site (2007–2013), JST site (2010–2014), CTR site (2012–2013), BHM site (2011–2013), OAK site (2010), and OLF site (2013) were presented. The model performance assessment exhibits the similar pattern at these six sites; thus, only results at the YRK agricultural–rural site are presented in this paper. The comparison between model predictions and measurements at the YRK site is shown in Figure 2.

As can be seen from Figure 2, in general, the ISORROPIA II model is able to reproduce  $NH_3$ ,  $HNO_3$ ,  $NH_4^+$ , and  $NO_3^-$  concentrations at the YRK site, with  $R^2$  values above 0.79. As for  $NH_3$  and  $NH_4^+$ , the slopes are 1.00 and 0.99, respectively, which indicate that the ISORROPIA II model predicts  $NH_3$  and  $NH_4^+$  well. However, for  $HNO_3$  and  $NO_3^-$ , the ISORROPIA II model tends to underpredict  $HNO_3$  (slope is 0.97), and overpredict  $NO_3^-$  (slope is 1.16), especially when the measured concentrations of  $HNO_3$  and  $NO_3^-$  are below  $4 \mu g m^{-3}$ . Some disagreement between model prediction and measurements can be observed. In this research, we explore the impact of ambient T and RH, model setups, NVCs, and OA on model performance, and the following sections show the results.

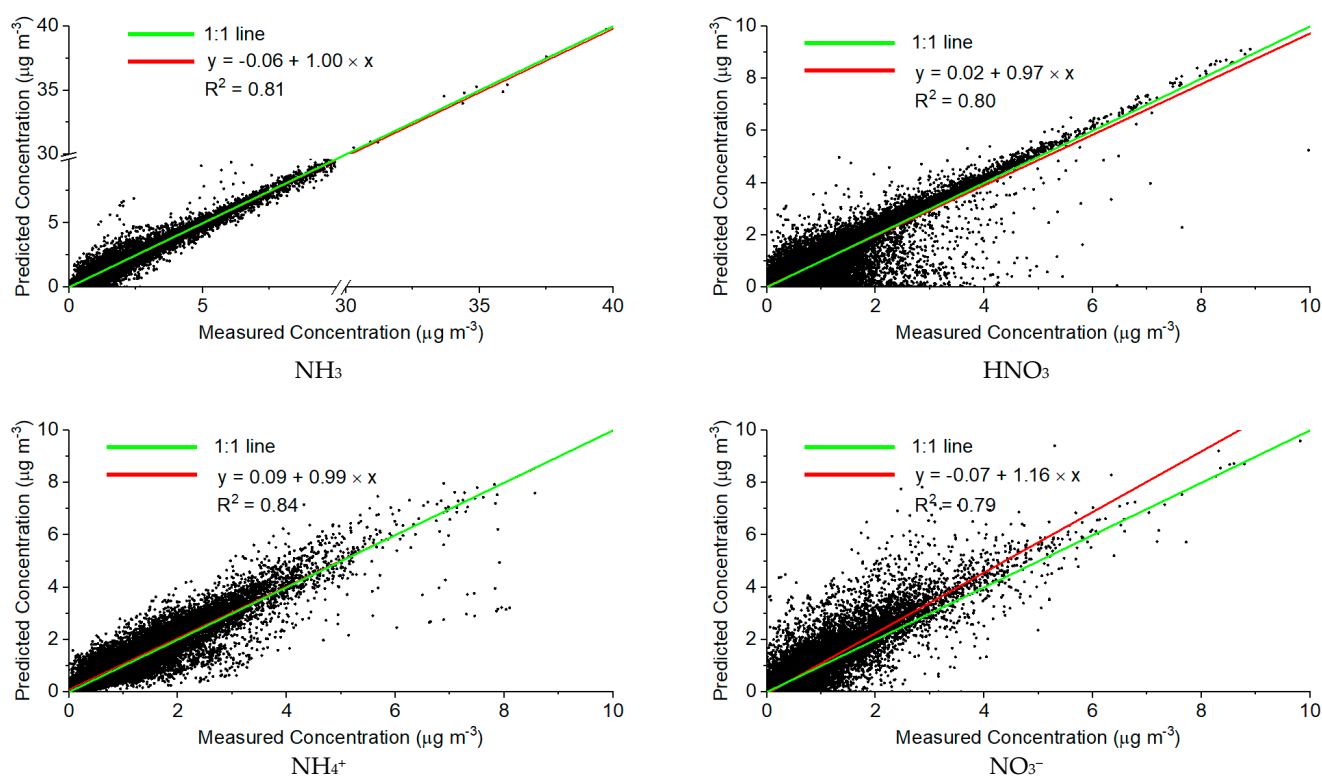


**Figure 2.** The comparison of prediction and observation using stable setup at the YRK site.

### 3.1.1. Ambient T-RH, Aerosol pH, and ISORROPIA II Stable and Metastable Setups

The impact of T and RH on model performance exhibits similar results at the six sites. Figures 3–5 show the ratios of prediction over observation ( $C_p/C_o$ ) at the YRK site using stable and metastable model setups.

As it can be seen from Figures 3–5, under  $T > 10$  °C and  $RH < 60\%$  conditions, ISORROPIA II model tends to excessively partition N into a gas phase, i.e., to overpredict HNO<sub>3</sub> and underpredict NO<sub>3</sub><sup>-</sup>. As for the prediction of iPM<sub>2.5</sub> (SO<sub>4</sub><sup>2-</sup> + NH<sub>4</sub><sup>+</sup> + NO<sub>3</sub><sup>-</sup>), generally, the ISORROPIA II model predicts the concentration of iPM<sub>2.5</sub> well; most of the  $C_p/C_o$  are within the range of 0.8 and 1.2. The accuracy of the prediction of iPM<sub>2.5</sub> is determined by three chemical compositions: SO<sub>4</sub><sup>2-</sup>, NH<sub>4</sub><sup>+</sup>, and NO<sub>3</sub><sup>-</sup>. One of the assumptions made by the ISORROPIA II model is that the vapor pressure of H<sub>2</sub>SO<sub>4</sub> is low; thus, all the H<sub>2</sub>SO<sub>4</sub> partitions into aerosol phase. The ISORROPIA II model always predicts SO<sub>4</sub><sup>2-</sup> concentration well; if SO<sub>4</sub><sup>2-</sup> accounts for the most of iPM<sub>2.5</sub> mass concentration, then the prediction of iPM<sub>2.5</sub> is not sensitive to the disagreement between predictions and measurements for NO<sub>3</sub><sup>-</sup> and NH<sub>4</sub><sup>+</sup>. The analyses of the mass closure of PM<sub>2.5</sub> in 2001–2016 at the agricultural–rural site, YRK, and industrial–residential site, JST, indicate that iPM<sub>2.5</sub> (SO<sub>4</sub><sup>2-</sup> + NH<sub>4</sub><sup>+</sup> + NO<sub>3</sub><sup>-</sup>) was the dominant components of PM<sub>2.5</sub> mass concentration before 2011, while in 2012–2016, the mass fraction of iPM<sub>2.5</sub> was decreased and organic carbon matter (OCM) dominated in PM<sub>2.5</sub> mass concentration. Among the three major chemical compositions of iPM<sub>2.5</sub>, SO<sub>4</sub><sup>2-</sup> accounted for greater than 59% of iPM<sub>2.5</sub>, which may explain the acceptable performance of ISORROPIA II in the prediction of iPM<sub>2.5</sub> concentration.

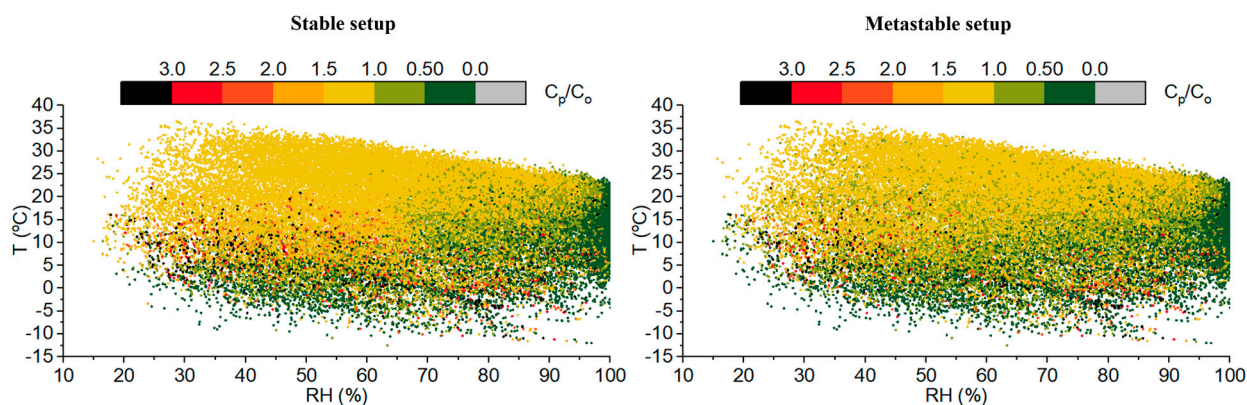


Figure 3. The ratios of  $C_p/C_o$  for  $\text{HNO}_3$  prediction using stable and metastable model setups.

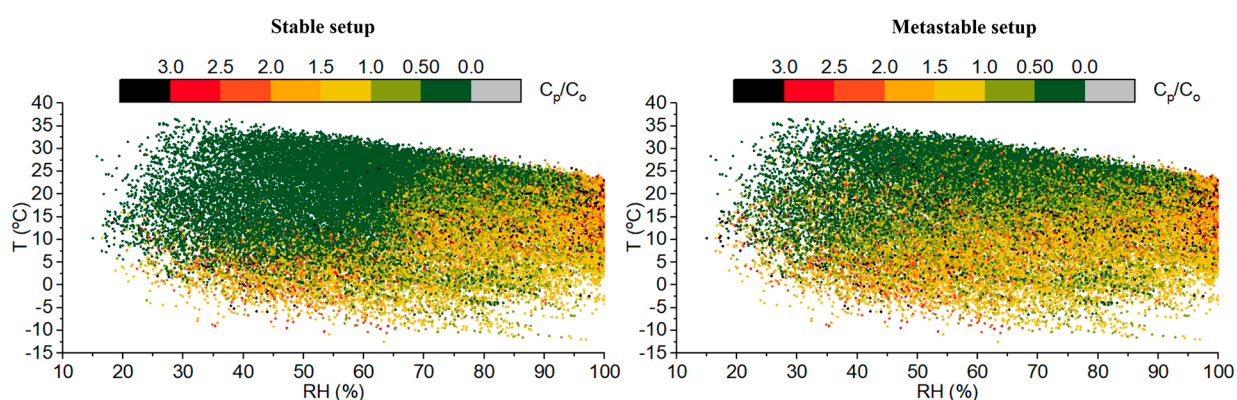


Figure 4. The ratios of  $C_p/C_o$  for  $\text{NO}_3^-$  using stable and metastable model setups.

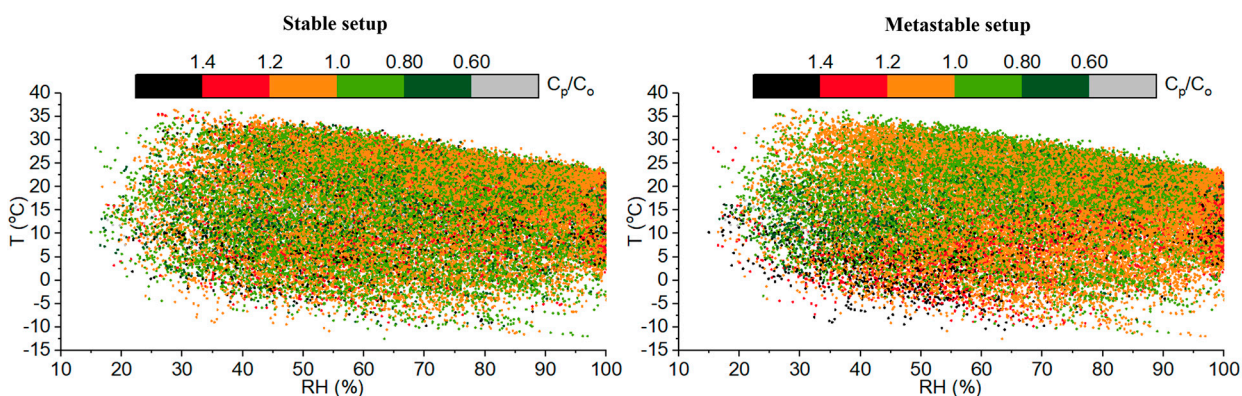
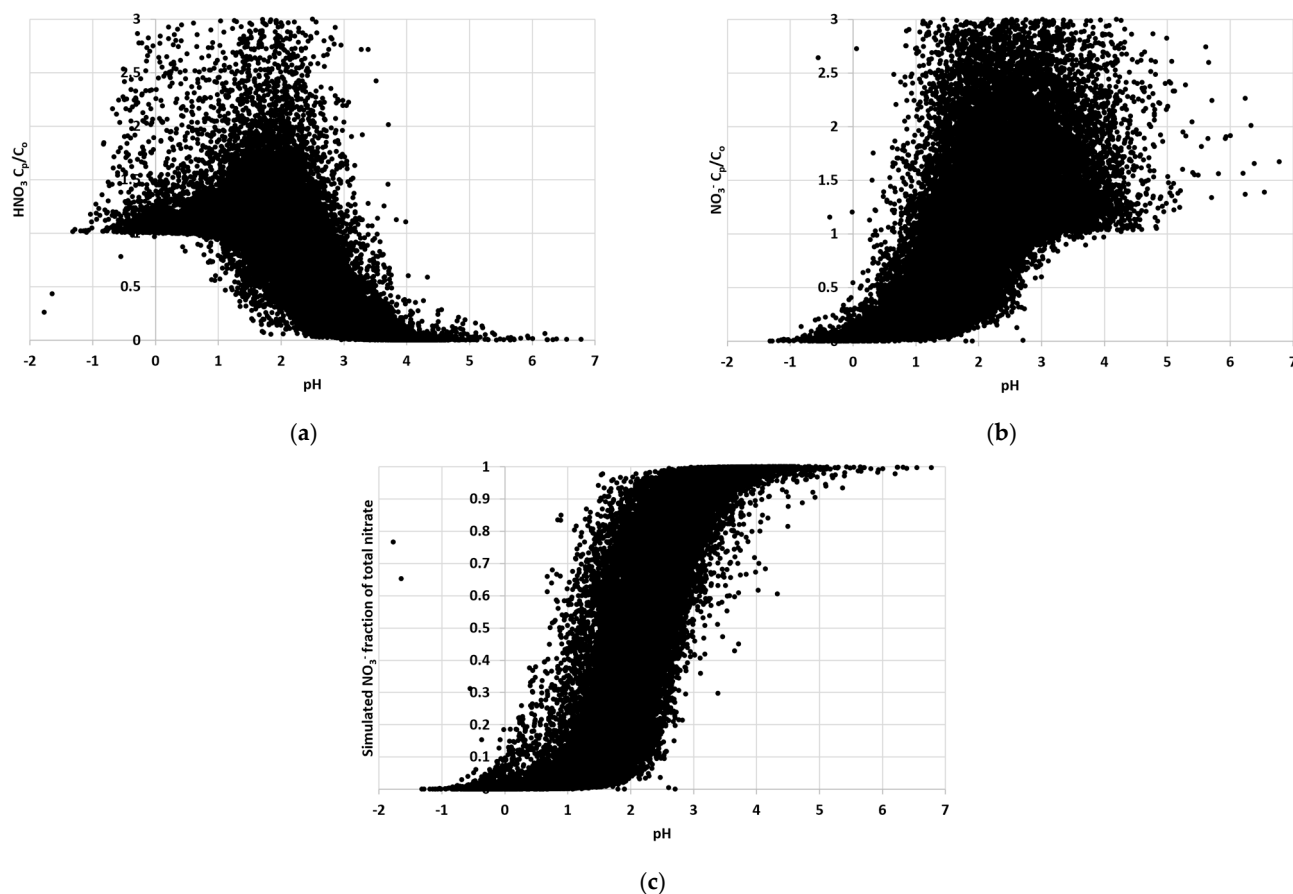


Figure 5. The ratios of  $C_p/C_o$  for  $\text{iPM}_{2.5}$  ( $\text{SO}_4^{2-} + \text{NH}_4^+ + \text{NO}_3^-$ ) using stable and metastable model setups.

The impact of pH on the under and overprediction of nitrate partitioning was shown below.

As seen in Figure 6a,b, when pH is less than 1, ISORROPIA II tends to overpredict  $\text{HNO}_3$  and underpredict  $\text{NO}_3^-$ ; when pH is greater than 3, ISORROPIA II tends to underpredict  $\text{HNO}_3$  and overpredict  $\text{NO}_3^-$ . The under and overprediction of nitrate partitioning is caused by the sensitivity of the simulated  $\text{NO}_3^-$  fraction of total nitrate ( $\epsilon(\text{NO}_3^-)$ ) to the change of pH. As seen in Figure 6c, when pH is less than 1 and greater than 3,  $\epsilon(\text{NO}_3^-)$  tends not to be sensitive to the change of pH (less than 10% change in  $\epsilon(\text{NO}_3^-)$ ); while when pH is in the range of 1 and 3, the change in pH may have significant impact on the nitrate partitioning. Thus, both under and overprediction of nitrate partitioning is observed when pH is in the range of 1 and 3.



**Figure 6.** The relationship of under and overprediction of nitrate partitioning with pH at the YRK site, (a)  $\text{HNO}_3 \text{ C}_p/\text{C}_0$  ratio under different pH; (b)  $\text{NO}_3^- \text{ C}_p/\text{C}_0$  ratio under different pH; (c) Simulated  $\text{NO}_3^-$  fraction of total nitrate under different pH.

### 3.1.2. Statistical Tests of Model Performance under Different T-RH Conditions

As for  $\text{NH}_3$  and  $\text{NH}_4^+$ , overprediction and underprediction both happen under all T-RH conditions. To quantitatively assess the performance of ISORROPIA II under different T-RH conditions, under each  $5^\circ\text{C T} \times 10\% \text{ RH}$  condition, the model performance (only the values of FB are shown) in the prediction of  $\text{NH}_3$ ,  $\text{NH}_4^+$ ,  $\text{HNO}_3$ ,  $\text{NO}_3^-$ , and  $\text{iPM}_{2.5}$  at the YRK site was assessed. The data at the JST site exhibit the similar results; thus, the statistical analysis results at the JST site are not shown here. We only show the values of FB for  $\text{NO}_3^-$  prediction with stable setup at the YRK site (Table 2); the results for the other gas- and particle-phase pollutants are in the supplemental material, Tables S1–S5.

For the comparison between the model performance with stable and metastable model setups, four parameters reveal the same conclusion about the selection of model setups under various T-RH conditions. The FB value can not only indicate the model performance, the sign of the value can also indicate over and underpredictions, thus FB is used in the model performance assessment discussion. As it can be seen from Tables S1 and S3, the performance of ISORROPIA II in the prediction of  $\text{NH}_3$  and  $\text{NH}_4^+$  is generally acceptable. While Table 2 indicates that prediction of  $\text{HNO}_3$  and  $\text{NO}_3^-$  is not satisfactory under certain T-RH conditions, especially under higher T and lower RH conditions, the ISORROPIA II model exhibits worse performance. The prediction of  $\text{iPM}_{2.5}$  is acceptable under all T-RH conditions. The model performance in the prediction of  $\text{HNO}_3$  and  $\text{NO}_3^-$  is sensitive to the dominant physical state (gas or aerosol) of  $\text{HNO}_3$  in ambient air. Under high T ( $>15^\circ\text{C}$ ) and low RH ( $<60\%$ ) conditions, the ammonium nitrate ( $\text{NH}_4\text{NO}_3$ ) may decompose into gas-phase  $\text{NH}_3$  and  $\text{HNO}_3$  due to the semi-volatile characteristic of  $\text{NH}_4\text{NO}_3$ , leading to the dominance of gas-phase  $\text{HNO}_3$  [8]; thus, most of the total  $\text{HNO}_3$  is in gas phase,

and the  $\text{NO}_3^-$  is more sensitive to the prediction uncertainties. The FB values for  $\text{NO}_3^-$  under  $T > 25^\circ\text{C}$  and  $\text{RH} < 70\%$  are all negative, as small as  $-2$ , which indicates extreme underprediction. While under low  $T$  or high  $\text{RH}$  conditions,  $\text{HNO}_3$  gas is underpredicted, especially for  $T < -5^\circ\text{C}$  or  $\text{RH} > 90\%$ . This can be explained by the fact that, under low  $T$  and/or high  $\text{RH}$  conditions, most of the  $\text{HNO}_3$  is in particle phase and the prediction of  $\text{HNO}_3$  gas is more sensitive to prediction uncertainties.

**Table 2.** Model performance assessment for  $\text{NO}_3^-$  prediction with stable setup at the YRK site.

Temperature	Relative Humidity							
	20–30%	30–40%	40–50%	50–60%	60–70%	70–80%	80–90%	90–100%
30–35 °C	<b>−2.00</b> <sup>M</sup>	<b>−2.00</b> <sup>M</sup>	<b>−2.00</b> <sup>M</sup>	<b>−1.98</b> <sup>M</sup>	<b>−1.81</b> <sup>M</sup>	NA	NA	NA
25–30 °C	<b>−2.00</b> <sup>M</sup>	<b>−2.00</b> <sup>M</sup>	<b>−2.00</b> <sup>M</sup>	<b>−1.99</b> <sup>M</sup>	<b>−1.66</b> <sup>M</sup>	<b>−0.71</b> <sup>M</sup>	<b>−0.48</b> <sup>S=M</sup>	NA
20–25 °C	<b>−2.00</b> <sup>M</sup>	<b>−1.95</b> <sup>M</sup>	<b>−1.84</b> <sup>M</sup>	<b>−1.97</b> <sup>M</sup>	<b>−1.10</b> <sup>M</sup>	<b>−0.27</b> <sup>M</sup>	<b>−0.09</b> <sup>M</sup>	0.25 <sup>S=M</sup>
15–20 °C	<b>−0.78</b> <sup>M</sup>	<b>−1.20</b> <sup>M</sup>	<b>−1.33</b> <sup>M</sup>	<b>−1.53</b> <sup>M</sup>	<b>−0.29</b> <sup>M</sup>	0.06 <sup>S</sup>	0.12 <sup>S</sup>	0.36 <sup>S=M</sup>
10–15 °C	<b>−0.65</b> <sup>M</sup>	<b>−0.61</b> <sup>M</sup>	<b>−0.49</b> <sup>S</sup>	<b>−0.47</b> <sup>M</sup>	<b>−0.02</b> <sup>S</sup>	0.30 <sup>S</sup>	0.29 <sup>S</sup>	0.41 <sup>S=M</sup>
5–10 °C	<b>−0.29</b> <sup>M</sup>	0.01 <sup>S</sup>	0.09 <sup>S</sup>	0.03 <sup>S</sup>	0.08 <sup>S</sup>	0.21 <sup>S</sup>	0.17 <sup>S</sup>	0.17 <sup>S=M</sup>
0–5 °C	0.18 <sup>S</sup>	0.30 <sup>S</sup>	0.29 <sup>S</sup>	0.25 <sup>S</sup>	0.12 <sup>S</sup>	0.09 <sup>S</sup>	0.07 <sup>S</sup>	0.17 <sup>S=M</sup>
−5–0 °C	NA	0.40 <sup>S</sup>	0.44 <sup>S</sup>	0.30 <sup>S</sup>	0.16 <sup>S</sup>	0.08 <sup>S</sup>	0.06 <sup>S</sup>	0.13 <sup>S=M</sup>
−10–−5 °C	NA	NA	NA	0.37 <sup>S</sup>	0.20 <sup>S</sup>	0.05 <sup>S</sup>	0.02 <sup>S</sup>	NA

<sup>a</sup> The unacceptable FB values ( $< -0.5$  or  $> 0.5$ ) are labeled as bold values; <sup>b</sup> NA: not applicable; <sup>c</sup> the FB values closer to 0 indicates the better model performance. The S superscript indicates the stable setup performs better, the M superscript indicates the metastable setup performs better, and the S = M superscript indicates the same model performance.

To further investigate the partitioning of  $\text{NH}_3\text{-NH}_4^+$  and  $\text{HNO}_3\text{-NO}_3^-$ , the measured gas-phase  $\text{NH}_3$  and  $\text{HNO}_3$  molar fractions under different T-RH conditions are shown in Figure 7.

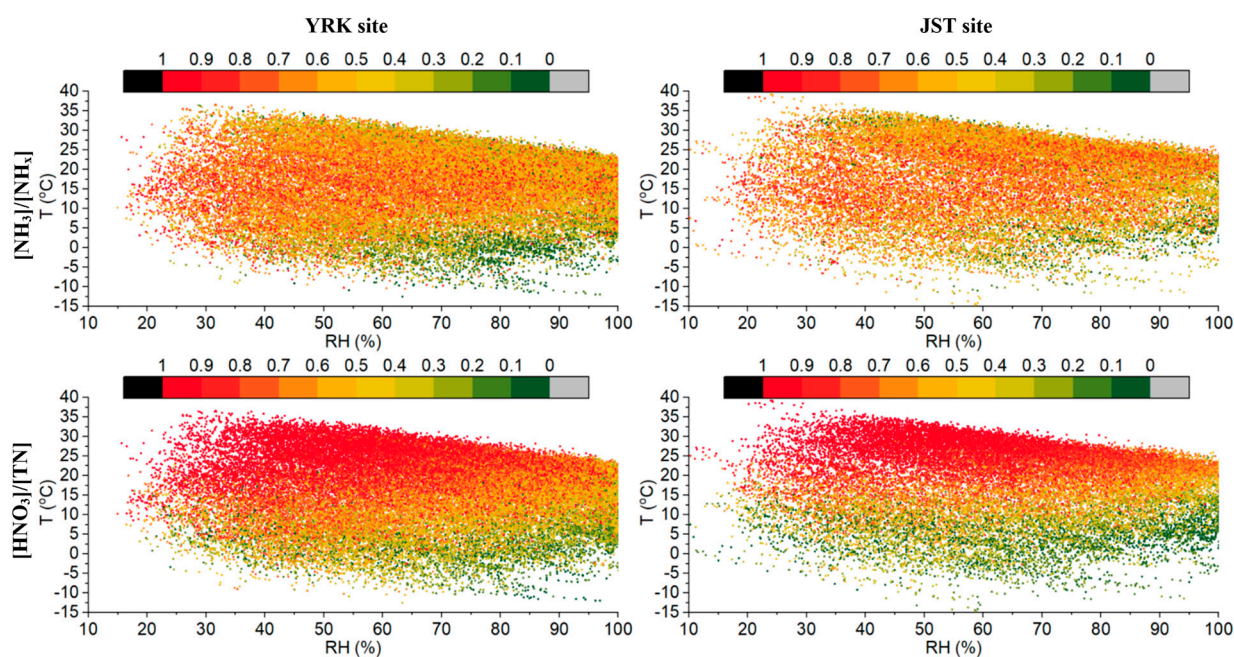


**Figure 7.** The measured gas-phase  $\text{NH}_3$  and  $\text{HNO}_3$  molar fractions under different T-RH conditions at the YRK and JST sites.

As for  $\text{NH}_3$ , Table S1 shows that the values of FB are closer to 0 under  $T > 5^\circ\text{C}$  than under  $T < 5^\circ\text{C}$ , and this indicates that the model performance of ISORROPIA II is better under  $T > 5^\circ\text{C}$  than under  $T < 5^\circ\text{C}$ . The semi-volatile characteristic of  $\text{NH}_4\text{NO}_3$  can lead to greater gas-phase  $\text{NH}_3$  molar fraction under high T. When the gas-phase  $\text{NH}_3$  dominates in the partitioning of  $\text{NH}_3\text{-NH}_4^+$ , the  $\text{NH}_4^+$  is more sensitive to prediction uncertainty and vice versa. The model performance in the prediction of  $\text{NH}_3$  is better under  $T > 5^\circ\text{C}$  conditions for both stable and metastable model setups. The predominance of one phase (aerosol or gas) of semi-volatile compounds under certain T-RH conditions can amplify the small errors in the model prediction of the other phase. The variable sensitivities to the prediction errors for gas-phase and particle-phase pollutants are more apparent for the partitioning of  $\text{HNO}_3\text{-NO}_3^-$ . As for  $\text{HNO}_3$ , Figure 7 indicates that, under  $T > 15^\circ\text{C}$  and  $\text{RH} < 90\%$  conditions, most of the  $\text{HNO}_3$  stays in the gas phase. The particle-phase  $\text{NO}_3^-$  only accounts for a small fraction of total available  $\text{HNO}_3$ ; the mass conservation of the  $\text{HNO}_3$  renders the  $\text{NO}_3^-$  concentration more sensitive to the uncertainties in the prediction. On the contrary, under  $T < 5^\circ\text{C}$  conditions, most of the  $\text{HNO}_3$  stays in particle phase, the mass conservation of the  $\text{HNO}_3$  renders the  $\text{HNO}_3$  gas concentration more sensitive to the uncertainties in the prediction. The dependence of the partitioning of  $\text{HNO}_3\text{-NO}_3^-$  on the T and RH makes the prediction of  $\text{NO}_3^-$  tougher than the other chemical compositions of  $\text{iPM}_{2.5}$ .

According to Ansari and Pandis (2000) and Fountoukis et al., (2009) [32,54], under different T-RH conditions, the metastable and stable model setups may have different performances in the prediction of  $\text{NH}_3$ ,  $\text{HNO}_3$ ,  $\text{NH}_4^+$ ,  $\text{NO}_3^-$ , and  $\text{iPM}_{2.5}$  ( $\text{SO}_4^{2-} + \text{NH}_4^+ + \text{NO}_3^-$ ). The differences of predictions using stable and metastable model setups are shown in Figure 8.

As can be seen from Figure 8, under high RH ( $\text{RH} > 83\%$ ) conditions, there is no difference for model prediction of  $\text{NH}_3$ ,  $\text{HNO}_3$ ,  $\text{NH}_4^+$ ,  $\text{NO}_3^-$ , and  $\text{iPM}_{2.5}$  ( $\text{SO}_4^{2-} + \text{NH}_4^+ + \text{NO}_3^-$ ) between the stable and metastable model setups. The high RH facilitates the absorption of water vapor to the  $\text{iPM}_{2.5}$  particles; the particle always stays in the aqueous phase and there is no salts precipitation. Thus, the prediction of the stable and the metastable setups is the same. However, Tables S1–S4 indicate that, under certain T-RH conditions, stable and metastable model setups may have different performances in the prediction of  $\text{NH}_3$ ,  $\text{HNO}_3$ ,  $\text{NH}_4^+$ ,  $\text{NO}_3^-$ , and  $\text{iPM}_{2.5}$ . Under  $T > 10^\circ\text{C}$  and  $\text{RH} < 60\%$  conditions, the ISORROPIA II model with metastable setup tends to perform better in the prediction of  $\text{NH}_3$ ,  $\text{HNO}_3$ ,  $\text{NH}_4^+$ ,  $\text{NO}_3^-$ , and  $\text{iPM}_{2.5}$ . Under  $T < 5^\circ\text{C}$  and  $\text{RH} < 90\%$  conditions, the ISORROPIA II model with stable setup tends to perform better in the prediction of  $\text{NH}_3$ ,  $\text{HNO}_3$ ,  $\text{NH}_4^+$ ,  $\text{NO}_3^-$ , and  $\text{iPM}_{2.5}$ . This can be explained by the difference in the prediction of the partitioning of  $\text{NH}_3\text{-NH}_4^+$  and  $\text{HNO}_3\text{-NO}_3^-$  by stable and metastable model setups.

As for  $\text{NH}_4^+$ , when  $\text{RH} < 80\%$ , the prediction of  $\text{NH}_4^+$  can be divided into four regions based on the difference between stable and metastable model setups. When  $T > 25^\circ\text{C}$ ,  $70\% < \text{RH} < 80\%$ , or  $T < 5^\circ\text{C}$ , the  $\text{NH}_4^+$  prediction of stable setup tends to be either greater or smaller than the metastable setup. When  $5^\circ\text{C} < T < 25^\circ\text{C}$  and  $\text{RH} < 70\%$ , the  $\text{NH}_4^+$  prediction of stable setup tends to be smaller than the metastable setup. As for  $\text{NO}_3^-$ , when  $\text{RH} < 80\%$ , the prediction of  $\text{NO}_3^-$  can be divided into three regions based on the difference between stable and metastable model setups. When  $70\% < \text{RH} < 80\%$ , the  $\text{NO}_3^-$  prediction of stable setup tends to be either greater or smaller than the metastable setup. When  $\text{RH} < 70\%$ , the  $\text{NO}_3^-$  prediction of stable setup tends to be either equal to or smaller than the metastable setup. Thus, the selection of stable and metastable model setups depends on ambient T and RH at the location.

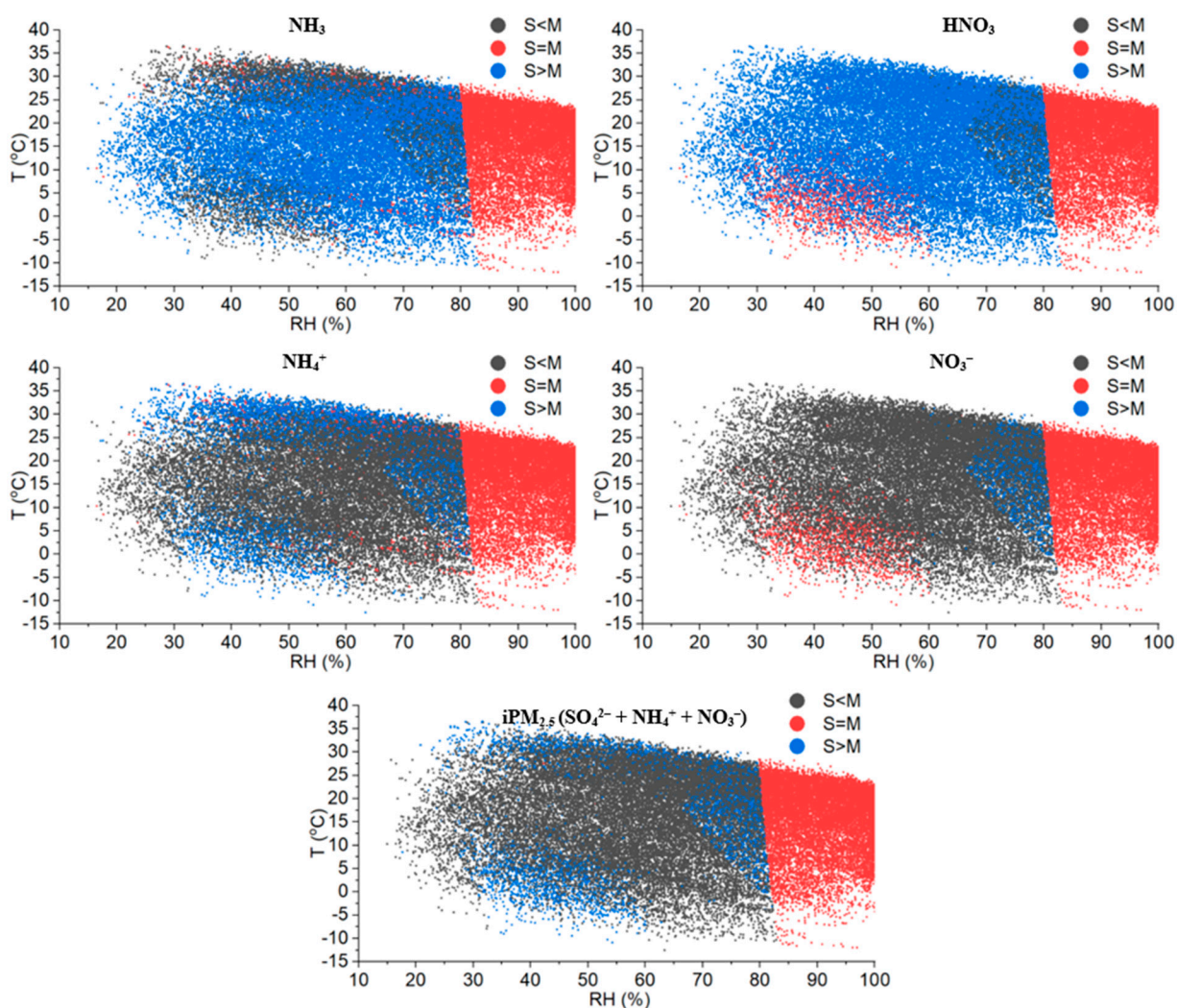


**Figure 8.** The difference of predictions using stable and metastable setups at the YRK site (S: stable; M: metastable).

The model performance of ISORROPIA II in simulating  $\text{NH}_3$  and  $\text{NH}_4^+$  under different GRs and measured charge balance is shown in the Figure 9.

As can be seen from Figure 9, when the measured charge balance is negative, the  $\text{NH}_3$  is underpredicted and  $\text{NH}_4^+$  is overpredicted; when  $\text{GR} < 1$ , the  $\text{NH}_3$  is underpredicted to a greater degree; when the measured charge balance is positive, the  $\text{NH}_3$  is over predicted and  $\text{NH}_4^+$  is underpredicted. In ambient air, the charge balance  $[\text{NH}_4^+] - 2 \times [\text{SO}_4^{2-}] - [\text{NO}_3^-]$  is equal to  $[\text{OH}^-] - [\text{H}^+] + [\text{organic anion}] + [\text{Cl}^-] - [\text{K}^+] - [\text{Na}^+] - 2 \times [\text{Ca}^{2+}] - 2 \times [\text{Mg}^{2+}]$ . However, only total  $\text{NH}_3$ , total  $\text{HNO}_3$ , and total  $\text{H}_2\text{SO}_4$  are the input data for ISORROPIA II in this research. In the model, the charge balance  $[\text{NH}_4^+] - 2 \times [\text{SO}_4^{2-}] - [\text{NO}_3^-]$  is equal to  $[\text{OH}^-] - [\text{H}^+]$ . Therefore, several possible reasons may explain the phenomena of over and underpredictions of  $\text{NH}_3$  and  $\text{NH}_4^+$ :

1. The measurement uncertainties in total  $\text{H}_2\text{SO}_4$  may explain part of the disagreement between predictions and measurements. Zhang et al., (2002) used 5 min measurements of  $\text{iPM}_{2.5}$  chemical compositions and their precursor gases to test the validity of the thermodynamic equilibrium assumption for the partitioning of  $\text{NH}_3$ - $\text{NH}_4^+$  [33]. Good agreement was found between field measurements and ISORROPIA II predictions in  $\text{NO}_3^-$  and  $\text{NH}_4^+$  when  $\sim 15\%$  downward correction in  $\text{SO}_4^{2-}$  concentration was applied. Yu et al., (2005) used different time resolution (5 min, 2 h, and 12 h) measurements of  $\text{NH}_3$ ,  $\text{NH}_4^+$ ,  $\text{HNO}_3$ ,  $\text{NO}_3^-$ , and  $\text{SO}_4^{2-}$  to assess the ability of ISOR-

ROPIA II in the prediction of  $\text{HNO}_3\text{-NO}_3^-$  partitioning. The sensitivity test indicated that the measurement uncertainties in the  $\text{SO}_4^{2-}$  and total  $\text{NH}_3$  concentrations may explain the errors in the prediction of  $\text{NO}_3^-$  [34].

2. The positive measured charge balance may be explained by the fact that part of the  $\text{NH}_4^+$  cations are associated with organic anions, which the ISORROPIA II model does not consider in the modeling system. In addition,  $\text{NH}_4^+$  cations may also be associated with  $\text{Cl}^-$ , which is not incorporated in the model input; the negative measured charge balance may be explained by the exclusion of the NVCs in the modeling system. Metzger et al., (2006) investigated the partitioning of  $\text{NH}_3\text{-NH}_4^+$  and  $\text{HNO}_3\text{-NO}_3^-$  using three thermodynamic models [55], the model performance was assessed with/without the inclusion of NVCs and organic acid ( $\text{R-COOH}$ ) in the input data. The comparison between model prediction and observations indicated that it is necessary to include NVCs and  $\text{R-COOH}$  in the model input of a thermodynamic model to accurately predict the gas-particle partitioning of  $\text{NH}_3\text{-NH}_4^+$  and  $\text{HNO}_3\text{-NO}_3^-$ .

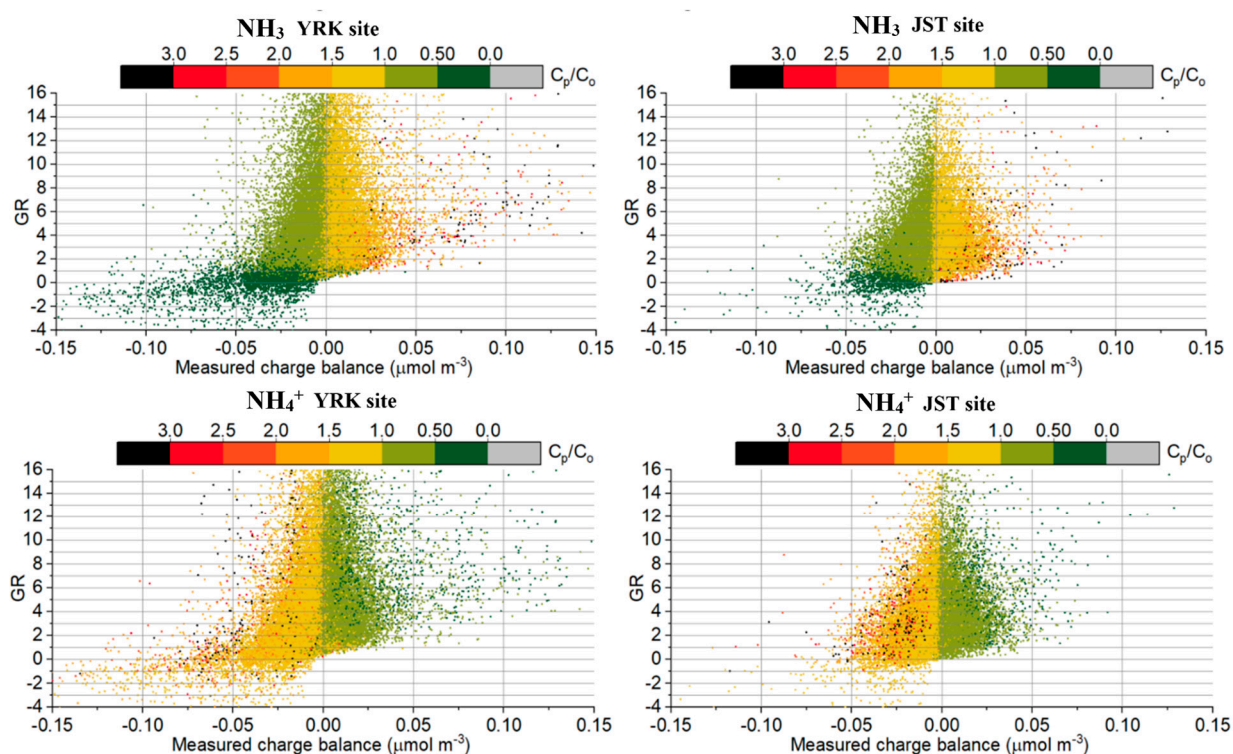


**Figure 9.** The ratios of prediction over observation for  $\text{NH}_3$  and  $\text{NH}_4^+$  using stable setup at the YRK and JST sites.

To further investigate the over and underprediction of gas-phase and particle-phase pollutants, the impact of NVCs on the model performance of ISORROPIA II was assessed.

### 3.1.3. Nonvolatile Cations (NVCs)

The comparisons between model predictions and measurements for particle-phase  $\text{NH}_4^+$  and  $\text{NO}_3^-$  at the YRK site are shown in Figure S1. As for daily measurements of particle-phase pollutants, in general, ISORROPIA II is able to reproduce the concentrations of  $\text{NH}_4^+$  and  $\text{NO}_3^-$ ; thus, factorial ANOVA statistical analysis is then used to check if NVCs (with/without nonvolatile cations) and model setups (stable/metastable setups) have significant impact on the prediction of  $\text{NH}_3$ ,  $\text{HNO}_3$ ,  $\text{NH}_4^+$ ,  $\text{NO}_3^-$ , and  $\text{iPM}_{2.5}$ . Only the data analysis results at the YRK site are shown in Table S6. Model setups and NVCs have variable impacts on the predictions of gas-phase and particle-phase pollutants. For  $\text{NH}_3$  prediction, only NVCs have significant impact on the model performance. For  $\text{NO}_3^-$

prediction, only model setup has significant impact on the model performance. For  $\text{HNO}_3$ ,  $\text{NH}_4^+$ , and  $\text{iPM}_{2.5}$  predictions, both NVCs and model setup have significant impact on the model performance.

To quantitatively assess the impact of NVCs and model setups on the model performance,  $F_{a2}$  and  $F_B$  values are calculated for model assessment at the YRK site (Table S7). Based upon the  $F_B$  values, inclusion of NVCs into the modeling framework and stable model setup has a better performance in the prediction of  $\text{NH}_3$ ,  $\text{HNO}_3$ ,  $\text{NH}_4^+$ ,  $\text{NO}_3^-$ , and  $\text{iPM}_{2.5}$  concentrations at the YRK site. Statistical summary of T and RH data at the YRK site indicates that, in the total 467 data points for the ISORROPIA II model assessment, 81 data points were under the  $T > 10^\circ\text{C}$  and  $\text{RH} < 60\%$  conditions, under which the metastable model setup has the better performance. In addition, 67 data points were under  $\text{RH} > 83\%$  condition, under which the performance of the model with stable and metastable setups is the same. The other data points were under conditions in which the stable setup has the better performance. This may indicate the preference of stable model setup at the YRK site. This finding is consistent with the study performed by [36], in which 6 h measurements of  $\text{NH}_3$ ,  $\text{HNO}_3$ ,  $\text{NH}_4^+$ ,  $\text{NO}_3^-$ , and  $\text{SO}_4^{2-}$  were used to assess the performance of ISORROPIA, and it was found that the inclusion of NVCs as equivalent  $\text{Na}^+$  can improve the model performance in the prediction of  $\text{NO}_3^-$  concentration. Therefore, the inclusion of the NVCs into the model framework is necessary to accurately simulate the thermodynamic equilibrium partitioning of  $\text{NH}_3\text{-NH}_4^+$ .

#### 3.1.4. Organic Aerosol (OA)

The relationships between the molar ratio-R and  $\text{OA}/\text{SO}_4^{2-}$  mass ratio at the YRK and JST sites are shown in Figure S2. There is a weak correlation between molar ratio-R and  $\text{OA}/\text{SO}_4^{2-}$  mass ratio,  $R^2 = 0.09$ , and  $0.17$  at the YRK and JST sites, respectively; the molar ratio-R slightly tends to decrease with  $\text{OA}/\text{SO}_4^{2-}$  mass ratio. As shown in Figure S2, no definite conclusion can be made about the impact of OA on the thermodynamic equilibrium partitioning of  $\text{NH}_3\text{-NH}_4^+$ . The higher  $\text{OA}/\text{SO}_4^{2-}$  mass ratio may indicate the lower probability for the uptake of  $\text{NH}_3$  by  $\text{H}_2\text{SO}_4$ . However, in this research, only a weakly negative correlation between molar ratio-R and  $\text{OA}/\text{SO}_4^{2-}$  mass ratio can be observed. One explanation may be that the daily data itself cannot adequately detect the impact of OA on the equilibrium process of  $\text{NH}_3\text{-NH}_4^+$  partitioning. Other factors such as T and RH can also affect the equilibrium process, while the coarse resolution of daily measurement cannot detect the variable sensitivities of the equilibrium process to the impacts of different factors. Thus, higher time resolution data such as 5 min data may be required to detect the impact of OA on the formation of  $\text{iPM}_{2.5}$ .

#### 3.2. Possible Reasons for the Disagreement between Model Predictions and Measurements

In assessment of the ISORROPIA II model performance under different T-RH-model setups conditions, it is discovered that ambient T and RH, model setups, and NVCs have significant impacts on model prediction. The inclusion of NVCs in the ISORROPIA II input is necessary to improve the model performance. Under certain T and RH conditions, ISORROPIA II tends to over or underpredict specific gas-phase or particle-phase pollutants. The stable and metastable model setups may also perform differently under different T-RH conditions. The impact of OA on the equilibrium assumption may not be detected by daily measurements; further research is needed to study the impact of OA on the equilibrium partitioning of  $\text{NH}_3\text{-NH}_4^+$ . The disagreement between model prediction and field measurements may be due to the following reasons:

1. The hourly and daily data were used in this research to assess the performance of the ISORROPIA II model. The duration of the daily input data may not be adequate to detect the impact of atmospheric transport and ambient T and RH on the thermodynamic equilibrium partitioning of  $\text{NH}_3\text{-NH}_4^+$ . Thus, the daily data of  $\text{NH}_3$ ,  $\text{HNO}_3$ , T, and RH may not be able to represent the thermodynamic equilibrium state of the gas-particle partitioning process.

2. The gas-particle system was not in a chemical equilibrium state. The mixture of  $PM_1$  and  $PM_{1-2.5}$  in secondary  $iPM_{2.5}$  may hinder the applicability of the ISORROPIA II model. The simple thermodynamic equilibrium assumption for  $iPM_{2.5}$  may not adequately characterize the partitioning of  $NH_3-NH_4^+$  in ambient air.
3. The inorganic  $PM_{2.5}$  particles were assumed to be internally mixed; therefore, the particles were treated as an ensemble bulk. However, Koo et al., (2003) observed that dynamic model may perform better in the prediction of  $iPM_{2.5}$  chemical compositions. The dynamic change of particle size distribution may require vigorous treatment of different physical processes such as condensation, evaporation, and coagulation. The size-resolved measurements with high time resolution are not available in this research, thus the dynamic approach cannot be tested.
4. Field measurement uncertainty. These uncertainties can be divided into two aspects: the measurement uncertainties caused by instruments and techniques, and the uncertainties caused by the atmospheric transport of air mass. The values below the instrument's detection limit were included in the ISORROPIA II model assessment; this may cause some disagreement between model predictions and measurements. The small values are especially sensitive to the prediction uncertainty. In addition, the ideal assessment of ISORROPIA II prediction skill should be based on the high time resolution measurements under controlled conditions. Furthermore, the thermodynamic equilibrium models should simulate the equilibrium partitioning of  $NH_3-NH_4^+$  and  $HNO_3-NO_3^-$  happening in the same air parcel. While in the field, air parcels laden with different concentrations of gas-phase and particle-phase pollutants may travel from and to any direction. Thus, the average measurements in one hour or day may not represent the thermodynamic equilibrium state of the same air parcel.
5. The history of RH experienced by air mass from different wind directions is not a priori; thus, the decision regarding the selection of stable and metastable setups is quite difficult, and this may also add some uncertainties to the model simulation.

Although the ISORROPIA II performance in the prediction of  $iPM_{2.5}$  concentration under all T-RH conditions is acceptable in the southeast U.S. due to the dominance of  $SO_4^{2-}$  in the  $iPM_{2.5}$  concentration, it may perform differently in other regions where  $SO_4^{2-}$  is not dominant in the  $iPM_{2.5}$  concentration. The  $PM_{2.5}$  chemical compositions varied in spatial and temporal scales in the U.S. The  $PM_{2.5}$  chemical compositions such as  $SO_4^{2-}$  and  $NO_3^-$  exhibited inverse seasonal variation patterns in the eastern and western coastal areas of U.S.;  $SO_4^{2-}$  exhibited a spatial heterogeneity with higher mass fraction in the eastern U.S. and lower mass fraction in California [56–58]. Thus, the model performance of ISORROPIA II in the prediction of  $iPM_{2.5}$  may differ according to the spatial scale.

#### 4. Conclusions

Based on the hourly and daily measurements of gas-phase and particle-phase pollutants at the SEARCH Network, the performance of ISORROPIA II was assessed under different T-RH, model setups, and NVCs conditions. The impact of OA on the thermodynamic equilibrium partitioning of  $NH_3-NH_4^+$  was also evaluated. Ambient T and RH, model setups, and NVCs have significant impact on model prediction. The inclusion of NVCs in the ISORROPIA II input is necessary to improve the model performance. Under high T ( $>10$  °C) and low RH ( $<60\%$ ) conditions, ISORROPIA II tends to overpredict  $HNO_3$  concentration and underpredict  $NO_3^-$  concentration. The predominance of one phase (aerosol or gas) of a semi-volatile compound can amplify the small errors in the model prediction of the other phase. The model with stable and metastable setups may also perform differently under different T-RH conditions. Metastable model setups might perform better under high T ( $>10$  °C) and low RH ( $<60\%$ ) conditions, while stable model setups might perform better under low T ( $<5$  °C) conditions. Under high RH (RH  $> 83\%$ ) conditions, there is no difference in the model performance with stable and metastable setups. The dominance of  $SO_4^{2-}$  in the  $iPM_{2.5}$  concentration may explain the acceptable model performance of ISORROPIA II in the prediction of  $iPM_{2.5}$  under all T-RH conditions.

Furthermore, higher resolution data may be required to investigate the impact of OA on the thermodynamic equilibrium partitioning of  $\text{NH}_3\text{-NH}_4^+$ . This research provides systematic assessment of the ISORROPIA II model under different conditions. Future studies using ISORROPIA II for the prediction of partitioning of  $\text{NH}_3\text{-NH}_4^+$  and  $\text{HNO}_3\text{-NO}_3^-$  should consider the inclusion of NVCs, the under/overprediction of  $\text{NO}_3^-/\text{HNO}_3$ , the selection of stable/metastable model setups under different T-RH conditions, and spatiotemporal variations of  $\text{iPM}_{2.5}$  chemical compositions.

**Supplementary Materials:** The following supporting information can be downloaded at: <https://www.mdpi.com/article/10.3390/atmos13121977/s1>, Figure S1: The comparison of prediction and observation for  $\text{NH}_4^+$  and  $\text{NO}_3^-$  at the YRK site; Figure S2: The relationships between molar ratio-R and OA/ $\text{SO}_4^{2-}$  mass ratio at the YRK and JST sites; Table S1: Model performance assessment for  $\text{NH}_3$  prediction with stable and metastable setups at the YRK site; Table S2: Model performance assessment for  $\text{HNO}_3$  prediction with stable and metastable setups at the YRK site; Table S3: Model performance assessment for  $\text{NH}_4^+$  prediction with stable and metastable setups at the YRK site; Table S4: Model performance assessment for  $\text{NO}_3^-$  prediction with metastable setups at the YRK site; Table S5: Model performance assessment for  $\text{iPM}_{2.5}$  prediction with stable and metastable setups at the YRK site; Table S6: Factorial ANOVA test results at the YRK site; Table S7: Model performance of ISORROPIA II at the YRK site.

**Author Contributions:** Conceptualization, B.C. and L.W.-L.; methodology, B.C. and L.W.-L.; formal analysis, B.C., J.C., P.B. and L.W.-L.; writing—original draft preparation, B.C.; writing—review and editing, B.C. and L.W.-L.; funding acquisition, L.W.-L. All authors have read and agreed to the published version of the manuscript.

**Funding:** This study was supported in part by NSF Award No. CBET-1804720.

**Institutional Review Board Statement:** Not applicable.

**Informed Consent Statement:** Not applicable.

**Data Availability Statement:** Data are available upon request from Eric Edgerton, all the data are extracted from SEARCH program Dropbox link: <https://www.dropbox.com/sh/o9hxo4wlo97zpe/AACbm6LetQowrpUgX4vUxnoDa?dl=0> (accessed on 21 November 2022).

**Acknowledgments:** Great thanks to Eric Edgerton from ARA, Inc. for providing the SEARCH program data. We also want to express our gratitude to Nicholas Meskhidze for his important revision advice.

**Conflicts of Interest:** The authors declare no conflict of interest.

## References

1. USEPA. Health and Environmental Effects of Particulate Matter. Available online: <https://www.epa.gov/pm-pollution/health-and-environmental-effects-particulate-matter-pm> (accessed on 31 October 2022).
2. Pui, D.Y.H.; Chen, S.; Zuo, Z.  $\text{PM}_{2.5}$  in China: Measurements, sources, visibility and health effects, and mitigation. *Particuology* **2014**, *13*, 1–26. [[CrossRef](#)]
3. Xing, Y.; Xu, Y.; Lian, Y. The impact of  $\text{PM}_{2.5}$  on the human respiratory system. *J. Thorac. Dis.* **2016**, *8*, E69–E74. [[CrossRef](#)] [[PubMed](#)]
4. Allen, A.G.; Harrison, R.M.; Erismann, J.-W. Field measurements of the dissociation of ammonium nitrate and ammonium chloride aerosols. *Atmos. Environ.* **1989**, *23*, 1591–1599. [[CrossRef](#)]
5. Hildemann, L.M.; Russell, A.G.; Cass, G.R. Ammonia and nitric acid concentration in equilibrium with atmospheric aerosols: Experiment vs. theory. *Atmos. Environ.* **1984**, *18*, 1737–1750. [[CrossRef](#)]
6. Stelson, A.W.; Seinfeld, J.H. Relative humidity and temperature dependence of the ammonium nitrate dissociation constant. *Atmos. Environ.* **1982**, *16*, 983–992. [[CrossRef](#)]
7. Shiraiwa, M.; Zuend, A.; Bertram, A.K.; Seinfeld, J.H. Gas-particle partitioning of atmospheric aerosols: Interplay of physical state, non-ideal mixing and morphology. *Phys. Chem. Chem. Phys.* **2013**, *15*, 11441–11453. [[CrossRef](#)]
8. Seinfeld, J.H.; Pandis, S.N. *Atmospheric Chemistry and Physics: From Air Pollution to Climate Change*; John Wiley & Sons: New York, NY, USA, 2016; ISBN 978-1-118-94740-1.
9. Cheng, B.; Wang-Li, L.; Meskhidze, N.; Classen, J.; Bloomfield, P. Partitioning of  $\text{NH}_3\text{-NH}_4^+$  in the Southeastern U.S. *Atmosphere* **2021**, *12*, 1681. [[CrossRef](#)]

10. Saxena, P.; Hudischewskyj, A.B.; Seigneur, C. A comparative study of equilibrium approaches to the chemical characterization of secondary aerosols. *Atmos. Environ.* **1986**, *20*, 1471–1483. [[CrossRef](#)]
11. Tanner, R.L.; Marlow, W.H.; Newman, L. Chemical composition correlations of size-fractionated sulfate in New York City. *Am. Chem. Soc.* **1979**, *13*, 75–78. [[CrossRef](#)]
12. Tolocka, M.P.; Solomon, P.A.; Mitchell, W.; Norris, G.A.; Gemmill, D.B.; Wiener, R.W.; Vanderpool, R.W.; Homolya, J.B.; Rice, J. East versus west in the US: Chemical characteristics of PM<sub>2.5</sub> during the winter of 1999. *Aerosol Sci. Technol.* **2001**, *34*, 88–96. [[CrossRef](#)]
13. Walker, J.T.; Whittall, D.R.; Robarge, W.; Paerl, H.W. Ambient ammonia and ammonium aerosol across a region of variable ammonia emission density. *Atmos. Environ.* **2004**, *38*, 1235–1246. [[CrossRef](#)]
14. Cheng, B.; Wang-Li, L. Spatial and temporal variations of PM<sub>2.5</sub> in North Carolina. *Aerosol Air Qual. Res.* **2019**, *19*, 698–710. [[CrossRef](#)]
15. Cheng, B.; Wang-Li, L.; Meskhidze, N.; Classen, J.; Bloomfield, P. Spatial and temporal variations of PM<sub>2.5</sub> mass closure and inorganic PM<sub>2.5</sub> in the Southeastern U.S. *Environ. Sci. Pollut. Res.* **2019**, *26*, 33181–33191. [[CrossRef](#)] [[PubMed](#)]
16. Cheng, B. and Wang-Li, L. Responses of secondary inorganic PM<sub>2.5</sub> to precursor gases in an ammonia abundant area in North Carolina. *Aerosol Air Qual. Res.* **2019**, *19*, 1126–1138. [[CrossRef](#)]
17. Pye, H.O.T.; Nenes, A.; Alexander, B.; Ault, A.P.; Barth, M.C.; Clegg, S.L.; Collett, J.L., Jr.; Fahey, K.M.; Hennigan, C.J.; Herrmann, H.; et al. The acidity of atmospheric particles and clouds. *Atmos. Chem. Phys.* **2020**, *20*, 4809–4888. [[CrossRef](#)] [[PubMed](#)]
18. Ansari, A.S.; Pandis, S.N. Prediction of multicomponent inorganic atmospheric aerosol behaviour. *Atmos. Environ.* **1999**, *33*, 745–757. [[CrossRef](#)]
19. Zhang, Y.; Seigneur, C.; Seinfeld, J.H.; Jacobson, M.; Clegg, S.L.; Binkowski, F.S. A comparative review of inorganic aerosol thermodynamic equilibrium modules: Similarities, differences, and their likely causes. *Atmos. Environ.* **2000**, *34*, 117–137. [[CrossRef](#)]
20. Cheng, B. *Dynamics of Rural and Urban Atmospheric Chemical Conditions and Inorganic Aerosols*; North Carolina State University: Raleigh, NC, USA, 2018.
21. Ravishankara, A.R. Heterogeneous and multiphase chemistry in the troposphere. *Science* **1997**, *276*, 1058–1065. [[CrossRef](#)]
22. Wexler, A.S.; Seinfeld, J.H. Analysis of aerosol ammonium nitrate: Departures from equilibrium during SCAQS. *Atmos. Environ.* **1992**, *26*, 579–591. [[CrossRef](#)]
23. Moya, M.; Pandis, S.N.; Jacobson, M.Z. Is the size distribution of urban aerosols determined by thermodynamic equilibrium? An application to Southern California. *Atmos. Environ.* **2002**, *36*, 2349–2365. [[CrossRef](#)]
24. Fountoukis, C.; Nenes, A. ISORROPIA II: A computationally efficient thermodynamic equilibrium model for K<sup>+</sup>-Ca<sup>2+</sup>-Mg<sup>2+</sup>-NH<sub>4</sub><sup>+</sup>-Na<sup>+</sup>-SO<sub>4</sub><sup>2-</sup>-NO<sub>3</sub><sup>-</sup>-Cl<sup>-</sup>-H<sub>2</sub>O aerosols. *Atmos. Chem. Phys. Discuss.* **2007**, *7*, 1893–1939. [[CrossRef](#)]
25. Ansari, A.S.; Pandis, S.N. An analysis of four models predicting the partitioning of semi-volatile inorganic aerosol components. *Aerosol Sci. Technol.* **1999**, *31*, 129–153. [[CrossRef](#)]
26. Nenes, A.; Pilinis, C.; Pandis, S.N. ISORROPIA: A new thermodynamic equilibrium model for multiphase multicomponent inorganic aerosols. *Aqua. Geochem.* **1998**, *4*, 123–152. [[CrossRef](#)]
27. Nenes, A.; Pilinis, C.; Pandis, S.N. Continued development and testing of a new thermodynamic aerosol module for urban and regional air quality models. *Atmos. Environ.* **1999**, *33*, 1553–1560. [[CrossRef](#)]
28. Fountoukis, C.; Nenes, A.; Pandis, S.; Pilinis, C. ISORROPIA v2.1 Reference Manual. 2009. Available online: <https://www.epfl.ch/labs/lapi/wp-content/uploads/2018/12/ISORROPIA21Manual.pdf> (accessed on 21 November 2022).
29. Koo, B.; Gaydos, T.M.; Pandis, S.N. Evaluation of the equilibrium, dynamic, and hybrid aerosol modeling approaches. *Aerosol Sci. Technol.* **2003**, *37*, 53–64. [[CrossRef](#)]
30. Hu, X.-M.; Zhang, Y.; Jacobson, M.Z.; Chan, C.K. Coupling and evaluating gas/particle mass transfer treatments for aerosol simulation and forecast. *J. Geophys. Res.* **2008**, *113*, 1–20. [[CrossRef](#)]
31. Meng, Z.; Seinfeld, J.H. Time scale to achieve atmospheric gas-aerosol equilibrium for volatile species. *Atmos. Environ.* **1996**, *30*, 2889–2900. [[CrossRef](#)]
32. Fountoukis, C.; Nenes, A.; Sullivan, A.; Weber, R.; Van Reken, T.; Fischer, M.; Matias, E.; Moya, M.; Farmer, D.; Cohen, R.C. Thermodynamic characterization of Mexico City aerosol during MILAGRO 2006. *Atmos. Chem. Phys.* **2009**, *9*, 2141–2156. [[CrossRef](#)]
33. Zhang, J.; Chameides, W.L.; Weber, R.; Cass, G.; Orsini, D.; Edgerton, E.S.; Jongejan, P.; Slanina, J. An evaluation of the thermodynamic equilibrium assumption for fine particulate composition: Nitrate and ammonium during the 1999 Atlanta Supersite Experiment. *J. Geophys. Res.* **2002**, *107*, 8414. [[CrossRef](#)]
34. Yu, S.; Dennis, R.; Roselle, S.; Nenes, A.; Walker, J.; Eder, B.; Schere, K.; Swall, J.; Robarge, W. An assessment of the ability of three-dimensional air quality models with current thermodynamic equilibrium models to predict aerosol NO<sub>3</sub><sup>-</sup>. *J. Geophys. Res.* **2005**, *110*, D07S13. [[CrossRef](#)]
35. Takahama, S.; Wittig, A.E.; Vayenas, V.; Davidson, C.I.; Pandis, S.N. Modeling the diurnal variation of nitrate during the Pittsburgh Air Quality Study. *J. Geophys. Res.* **2004**, *109*, D16S06. [[CrossRef](#)]
36. Moya, M.; Ansari, A.S.; Pandis, S.N. Partitioning of nitrate and ammonium between the gas and particulate phases during the 1997 IMADA-AVER study in Mexico City. *Atmos. Environ.* **2001**, *35*, 1791–1804. [[CrossRef](#)]

37. Goetz, S.; Aneja, V.P.; Zhang, Y. Measurement, analysis, and modeling of fine particulate matter in Eastern North Carolina. *J. Air Waste Manag. Assoc.* **2008**, *58*, 1208–1214. [[CrossRef](#)]
38. Walker, J.T.; Robarge, W.P.; Shendrikar, A.; Kimball, H. Inorganic PM<sub>2.5</sub> at a U.S. agricultural site. *Environ. Pollut.* **2006**, *139*, 258–271. [[CrossRef](#)] [[PubMed](#)]
39. Silvern, R.F.; Jacob, D.J.; Kim, P.S.; Marais, E.A.; Turner, J.R. Inconsistency of ammonium-sulfate aerosol ratios with thermodynamic models in the eastern U.S.: A possible role of organic aerosol. *Atmos. Chem. Phys.* **2017**, *17*, 5107–5118. [[CrossRef](#)]
40. Gill, P.S.; Graedel, T.E.; Weschler, C.J. Organic films on atmospheric aerosol particles, fog droplets, cloud droplets, raindrops, and snowflakes. *Rev. Geophys.* **1983**, *21*, 903–920. [[CrossRef](#)]
41. Li, Q.-F.; Wang-Li, L.; Shah, S.B.; Jayanty, R.K.M.; Bloomfield, P. Ammonia concentrations and modeling of inorganic particulate matter in the vicinity of an egg production facility in Southeastern USA. *Environ. Sci. Pollut. Res.* **2014**, *21*, 4675–4685. [[CrossRef](#)]
42. Li, Q.-F.; Wang-Li, L.; Liu, Z.; Jayanty, R.K.M.; Shah, S.B.; Bloomfield, P. Major ionic composition of fine particulate matter in an animal feeding operation facility and its vicinity. *J. Air Waste Manag. Assoc.* **2014**, *64*, 1279–1287. [[CrossRef](#)]
43. Liggio, J.; Li, S.M.; Vlasenko, A.; Stroud, C.; Makar, P. Depression of ammonia uptake to sulfuric acid aerosols by competing uptake of ambient organic gases. *Environ. Sci. Technol.* **2011**, *45*, 2790–2796. [[CrossRef](#)]
44. Pye, H.O.T.; Zuend, A.; Fry, J.L.; Isaacman-VanWertz, G.; Capps, S.L.; Appel, K.W.; Foroutan, H.; Xu, L.; Ng, N.L.; Goldstein, A.H. Coupling of organic and inorganic aerosol systems and the effect on gas–particle partitioning in the southeastern US. *Atmos. Chem. Phys.* **2018**, *18*, 357–370. [[CrossRef](#)]
45. Guo, H.; Nenes, A.; Weber, R.J. The underappreciated role of nonvolatile cations on aerosol ammonium-sulfate molar ratios. *Atmos. Chem. Phys.* **2018**, *18*, 17307–17323. [[CrossRef](#)]
46. Zheng, G.; Su, H.; Wang, S.; Andreae, M.O.; Pöschl, U.; Cheng, Y. Multiphase buffer theory explains contrasts in atmospheric aerosol acidity. *Science* **2020**, *369*, 1374–1377. [[CrossRef](#)] [[PubMed](#)]
47. Electric Power Research Institute (EPRI). 2008. Available online: [https://yosemite.epa.gov/sab%5CSABPRODUCT.NSF/B99E5E7B1FC13632852575B50069AAC2/\\$File/EPRI-SEARCH+for+EPA+SAB+INC+May+14-15+2009+Meeting.pdf](https://yosemite.epa.gov/sab%5CSABPRODUCT.NSF/B99E5E7B1FC13632852575B50069AAC2/$File/EPRI-SEARCH+for+EPA+SAB+INC+May+14-15+2009+Meeting.pdf) (accessed on 21 November 2022).
48. Hansen, D.A.; Edgerton, E.S.; Hartsell, B.E.; Jansen, J.J.; Kandasamy, N.; Hidy, G.M.; Blanchard, C.L. The Southeastern Aerosol Research and Characterization Study: Part 1–Overview. *J. Air Waste Manag. Assoc.* **2003**, *53*, 1460–1471. [[CrossRef](#)] [[PubMed](#)]
49. Hidy, G.M.; Blanchard, C.L.; Baumann, K.; Edgerton, E.; Tanenbaum, S.; Shaw, S.; Knipping, E.; Tombach, I.; Jansen, J.; Walters, J. Chemical climatology of the Southeastern United States, 1999–2013. *Atmos. Chem. Phys.* **2014**, *14*, 11893–11914. [[CrossRef](#)]
50. Cohen, M.A.; Ryan, P.B. Observations less than the analytical limit of Detection: A new approach. *JAPCA* **1989**, *39*, 328–329. [[CrossRef](#)]
51. USEPA. Guidance for Data Quality Assessment. 2000. Available online: <https://www.epa.gov/sites/production/files/2015-06/documents/g9-final.pdf> (accessed on 21 November 2022).
52. Chang, J.C.; Hanna, S.R. Air quality model performance evaluation. *Meteo. Atmos. Phys.* **2004**, *87*, 167–196. [[CrossRef](#)]
53. Kumar, A.; Dixit, S.; Varadarajan, C.; Vijayan, A.; Masuraha, A. Evaluation of the AERMOD dispersion model as a function of atmospheric stability for an urban area. *Environ. Prog.* **2006**, *25*, 141–151. [[CrossRef](#)]
54. Ansari, A.S.; Pandis, S.N. The effect of metastable equilibrium states on the partitioning of nitrate between the gas and aerosol phases. *Atmos. Environ.* **2000**, *34*, 157–168. [[CrossRef](#)]
55. Metzger, S.; Mihalopoulos, N.; Levievel, J. Importance of mineral cations and organics in gas-aerosol partitioning of reactive nitrogen compounds: Case study based on MINOS results. *Atmos. Chem. Phys.* **2006**, *6*, 2549–2567. [[CrossRef](#)]
56. Bell, M.L.; Dominici, F.; Ebisu, K.; Zeger, S.L.; Samet, J.M. Spatial and temporal variation in PM<sub>2.5</sub> chemical composition in the United States for health effects studies. *Environ. Health Perspect.* **2007**, *115*, 989–995. [[CrossRef](#)]
57. Cheng, B.; Wang-Li, L.; Classen, J.; Meskhidze, N.; Bloomfield, P. Spatial and temporal variations of atmospheric chemical condition in the Southeastern U.S. *Atmos. Res.* **2021**, *248*, 105190. [[CrossRef](#)]
58. Hand, J.L.; Schichtel, B.A.; Pitchford, M.; Malm, W.C.; Frank, N.H. Seasonal composition of remote and urban fine particulate matter in the United States. *J. Geophys. Res.* **2012**, *117*, D05209. [[CrossRef](#)]